THE JOURNAL OF PHYSICAL CHEMISTRY Letters

Letter

pubs.acs.org/JPCL

Momentum-Dependent Lifetime Broadening of Electron Energy Loss Spectra: A Self-Consistent Coupled-Plasmon Model

J. D. Bourke and C. T. Chantler*

School of Physics, University of Melbourne, Parkville, Victoria 3010 Australia

ABSTRACT: The complex dielectric function and associated energy loss spectrum of a condensed matter system is a fundamental material parameter that determines both the optical and electronic scattering behavior of the medium. The common representation of the electron energy loss function (ELF) is interpreted as the susceptibility of a system to a single- or bulk-electron (plasmon) excitation at a given energy and momentum and is commonly derived as a summation of noninteracting free-electron resonances with forms constrained by adherence to some externally determined optical standard. This work introduces a new causally constrained momentum-dependent broadening theory, permitting a more physical representation of optical and electronic resonances that agrees more closely with both optical attenuation and electron scattering data. We demonstrate how the momentum dependence of excitation resonances may be constrained uniquely by utilizing a coupled-plasmon model, in which high-energy excitations are able to relax into lower-energy excitations within the medium. This enables a robust and fully self-consistent theory with no free or fitted parameters that reveals additional physical insight not present in previous work. The new developments are applied to the scattering behavior of solid molybdenum and aluminum. We find that plasmon and single-electron lifetimes are significantly affected by the presence of alternate excitation channels and show for molybdenum that agreement with high-precision electron inelastic mean free path data is dramatically improved for energies above 20 eV.

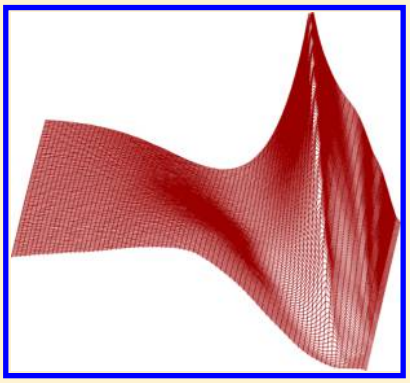

The low-energy inelastic scattering behavior of electrons in a medium is of fundamental and critical importance to many spectroscopies and microscopies used in modern materials analysis. Electron energy loss spectroscopy (EELS),[1] low-energy electron diffraction,[2] X-ray absorption spectroscopy,[3] and electron microscopy[4] all demand detailed knowledge of electron scattering, inelastic mean free paths (IMFPs), and the dielectric response of the medium being probed. This work aims to incorporate new physical processes into a causally constrained model of the dielectric response of materials in order to improve our understanding and quantification of critical material properties.

We are interested in developing theory to calculate the electron IMFP in the low-energy region (below ∼100 eV), where recent experimental results have demonstrated deficiencies in the established literature.[5,6] It has become apparent that existing models of the dielectric response of materials to low-energy electrons systematically overestimate the electron IMFP. Recent theoretical works suggest that this is due to either a poor account of single- and bulk-electron excitation lifetime broadening[7] or a lack of consideration for exchange and correlation effects in the dielectric theory of solids.[8] It is plausible that both of these effects contribute to the discrepancy, but without properly constrained theoretical models, it is not possible to definitively assess the contribution of each.

Attempts to resolve the discrepancy using variations in lifetime broadening parameters for optical resonances have shown that this approach may yield good agreement for energies higher than 50 eV. Recent work of this nature by Da et al. achieved particularly strong success with a model using many fitted resonance terms possessing both positive and negative oscillator strengths.[9] They were subsequently able to achieve excellent agreement with experimental results across all energies studied by using an additional empirical reduction parameter. Although successful, such an approach is ultimately insufficient, however, as it lacks a well-defined physical justification and utilizes an unconstrained representation of optical resonances that are constructed using a potentially overcomplete basis set.

This work focuses instead on the momentum dependence of the lifetime broadening of single-electron and bulk-electron (plasmon) excitations, developing an earlier discussion on the extension of the widely used optical data model for calculations of the electron energy loss function (ELF) and electron IMFP.[10] We will demonstrate how a model may be developed to incorporate these effects in both a physical and uniquely constrained way. These developments will be applied to the test cases of elemental molybdenum and aluminum, allowing us to probe their effects for a free-electron-like material with a single dominant resonance peak and a material with more complex band structure and many optical resonances. In the case of molybdenum, our improvements result in dramatic improve-

Received: November 8, 2014
Accepted: December 24, 2014

DOI: 10.1021/jz5023812
J. Phys. Chem. Lett. 2015, 6, 314−319

ment in the agreement with recent high-precision experimental results.

We begin with a review of the basic features of the optical data model. This approach has been developed over some decades from the original works of Penn[11] and Tung et al.,[12] and a version of this model is used in the work of Tanuma et al., who have constructed the most comprehensive and widely cited tabulations of IMFPs in the current literature.[13] The model deals with the determination of the electron ELF, which is the principal determinant of the electron IMFP λ following

$$\lambda(E)^{-1} = \frac{\hbar}{a_0 \pi E} \int_0^{(E-E_F)/\hbar} \int_{q_-}^{q_+} \frac{1}{q} \operatorname{Im}\left[\frac{-1}{\varepsilon(q,\omega)}\right] dq\, d\omega \tag{1}$$

The term $\operatorname{Im}[-1/(\varepsilon(q,\omega))]$ is the electron ELF and may be interpreted as a relative probability of an excitation of energy $\hbar\omega$ and momentum $\hbar q$ propagating in the medium.[14] The terms a_0 and m are the Bohr radius and electron mass, while the Fermi energy, E_F, is defined relative to the bottom of the conduction band. The limits of the momentum integral are given by

$$q\pm = \sqrt{\frac{2mE}{\hbar^2}} \pm \sqrt{\frac{2m}{\hbar^2}(E - \hbar\omega)} \tag{2}$$

Within this model, the problem of calculating the electron IMFP is reduced to that of calculating the momentum-dependent dielectric function $\varepsilon(q,\omega)$. This problem has been widely studied but has been solved satisfactorily only for the case of a nearly free-electron gas (FEG). In this instance, one may use the theory of Lindhard to define the resonant behavior of a lossless FEG[15] or the theory of Mermin, an extension to the Lindhard theory, for a more physical description inclusive of excitation lifetime broadening.[16] The commonly used classical Drude model is not considered here as it lacks any well-defined dispersion relation for low-energy electron excitations.[17]

The FEG theory must be extended to describe the behavior of a real solid with complex band structure. We therefore utilize the relatively greater availability of information regarding the optical limit of the dielectric function $\varepsilon(0,\omega)$. The optical dielectric function and optical ELF, $\operatorname{Im}[-1/(\varepsilon(0,\omega))]$, may be obtained directly using optical transmission or reflection measurements[18,19] or inferred from EELS or reflection EELS.[20] Recent developments have also enabled calculations of the optical ELF using density functional theory (DFT).[7,17] The optical data model posits that the momentum-dependent ELF of a solid may then be determined by constructing a sum of FEG-type resonances (Lindhard, Mermin, or otherwise) that match the optical behavior of the material, that is, the ELF in the limit $\hbar q \to 0$. Mathematically, we can write this condition as

$$\operatorname{Im}\left[\frac{-1}{\varepsilon_{\text{data}}(0,\omega)}\right] = \sum_i A_i \operatorname{Im}\left[\frac{-1}{\varepsilon_{\text{FEG}}(0,\omega;\omega_p=\omega_i)}\right] \tag{3}$$

where $\operatorname{Im}[-1/(\varepsilon_{\text{FEG}}(0,\omega;\omega_p=\omega_i))$ is the optical loss function for a FEG. This loss function will consist of a single resonance peak, situated in the optical limit at the plasma frequency $\omega_p = \omega_i$. The relative amplitudes A_i are defined by the match to the externally determined optical spectrum. If Lindhard-type functions are used to define the FEG, then each component resonance will be a delta function in the optical limit, and the A_i terms are uniquely defined

$$A_i = \frac{2}{\pi}\omega_i \Delta\omega \operatorname{Im}\left[\frac{-1}{\varepsilon_{\text{data}}(0,\omega_i)}\right] \tag{4}$$

where $\Delta\omega$ is the spacing between sampled points on the externally determined optical spectrum. If we then sum such component resonances using their full momentum-dependent forms, we arrive at a momentum-dependent ELF for the solid

$$\operatorname{Im}\left[\frac{-1}{\varepsilon(q,\omega)}\right] = \sum_i A_i \operatorname{Im}\left[\frac{-1}{\varepsilon_{\text{FEG}}(q,\omega;\omega_p=\omega_i)}\right] \tag{5}$$

This can then be integrated following eq 1 to evaluate the electron IMFP. The use of Lindhard terms to construct the electron ELF has been a common practice because it is uniquely constrained via eq 4 and because it can be used to match any optical dielectric function precisely. The Lindhard model is, however, unphysical due to its lack of broadening to account for the lifetime of the excitations that presents. This limitation led to the development of the Mermin function,[16] which expands on the Lindhard function in such a manner that it retains adherence to the causal constraints of the Thomas–Reiche–Kuhn and Kramers–Kronig sum rules.[21] The Mermin dielectric function, $\varepsilon_M(q,\omega,\gamma)$, is defined in relation to the Lindhard dielectric function, $\varepsilon_L(q,\omega)$, by the expression

$$\varepsilon_M(q,\omega,\gamma) = 1 + \frac{(1+i\gamma/\omega)[\varepsilon_L(q,\omega+i\gamma)-1]}{1+(i\gamma/\omega)[\varepsilon_L(q,\omega+i\gamma)-1]/[\varepsilon_L(q,0)-1]} \tag{6}$$

where γ is the broadening associated with the finite lifetime of a resonant excitation. The use of Mermin terms in the optical data model has become popular in recent times,[9,22,23] and in particular, it has been used to demonstrate that the observed discrepancies between theoretical and experimental IMFPs may be reduced significantly by the inclusion of plasmon broadening terms γ_i.[24] These Mermin-based optical data models are, however, still subject to a number of limitations in terms of both implementation and physicality.

The first such limitation is due to the matching of externally determined optical loss data via eq 3. Because the Mermin functions generally possess a finite width, one cannot always guarantee a precise match to an arbitrary optical loss spectrum. The negative oscillator approach of Da et al. provides a way to overcome this limitation,[9] but in doing so, it generates a large number of unconstrained resonance terms, which in turn exacerbate another problem with the Mermin representation—that of uniqueness.

Any Mermin-type fit to an optical ELF has many free parameters— the number of oscillators, the plasma frequency ω_i of each, their relative amplitudes A_i, and their widths γ_i. Therefore, it is easy to see that one may readily generate many quite different sets of parameters that all closely represent the observed or nominal optical loss spectrum. These different representations lead to very different electron ELFs and therefore very different conclusions regarding the electron IMFP. The more Mermin terms used in order to refine the fit, the worse this problem can become.

Mermin fitting approaches also suffer from physical limitations. For instance, the representation of the electron

DOI: 10.1021/jz5023812
J. Phys. Chem. Lett. 2015, 6, 314–319

oscillators usually involves the use of a single broadening parameter γ_i for each excitation. In reality, the lifetime of an excitation is dependent not only on its energy but on its momentum, and therefore, the use of a single parameter for this purpose is insufficient.

Some early works attempted to quantify the momentum dependence of plasmon broadening but were strongly hampered by the inability to properly describe the full excitation spectrum for non-free-electron-like materials.[25,26] More modern works have investigated the problem from a phenomenological point of view[27] and demonstrated some success with the use of fitted relationships for the momentum dependence of excitation lifetimes.[28] A robust physical determination of lifetimes has been lacking, however, and recent investigations using first-principles DFT have shown success only in very limited regions of energy and momenta[29,30]

An even more severe problem associated with optical data modeling is the universally used initial assumption that the solid is a sum of noninteracting FEG resonance terms. Clearly, all of the electrons in a solid can interact, and therefore, each excitation channel must be affected by all of the other resonances of the material.

In light of these limitations, we present a new model based on a self-consistent Mermin representation with momentum-dependent broadening widths $\gamma_i(q)$. The first step, as in all optical data models, is to determine the spectrum at $\hbar q = 0$. In order to solve the problems of uniqueness and precise spectrum matching, we define the following condition for all excitations i

$$\lim_{q\to 0} \gamma_i(q) = 0 \tag{7}$$

This reduces the optical behavior to the equivalent of a Lindhard model, which is uniquely constrained by eq 4. While the use of Lindhard terms is not physical in general, we note that this reduction to Lindhard behavior is permissible as the optical limit as defined is an idealization that does not apply to any real physical system. In fact, we will show that such a reduction is even *predicted* by a self-consistent dielectric model.

The next problem is to specify the form of the values for $\gamma_i(q)$. In our preliminary investigation prior to this work,[10] the Kramers–Kronig and Thomas–Reiche–Kuhn sum rules were used to constrain momentum-dependent broadening values within a FEG toy model. When using Mermin functions, however, these sum rules are automatically satisfied for all broadening values. Further, a Mermin model where $\gamma_i(q) = 0, \forall i$ always satisfies the sum rule given by eq 12 of[10]

$$\frac{1}{\omega_q}\int_0^\infty \omega\,\mathrm{Im}\left[\frac{-1}{\varepsilon(q,\omega)}\right]\mathrm{d}\omega = \omega_q\int_0^\infty \frac{1}{\omega}\,\mathrm{Im}\left[\frac{-1}{\varepsilon(q,\omega)}\right]\mathrm{d}\omega \tag{8}$$

These properties are highly desirable for our model because the momentum-dependent lifetime broadening of excitations must be determined from the dielectric behavior of the material itself. Such an approach solves not only the problem of specifying $\gamma_i(q)$ but also the problem of accounting for interactions between excitation channels. We have seen that for a free particle, an IMFP may be evaluated using eq 1. We may readily use the same formalism to derive an effective IMFP for a bound particle, provided that we assign appropriate limits to the momentum integral. In this case, we use the standard relationship $(\hbar^2q^2/2m) = \hbar\omega$ to generalize the expression for new momentum limits $q^*\pm$ to

$$q^*\pm = \sqrt{\frac{q^2}{\hbar\omega}E} \pm \sqrt{\frac{q^2}{\hbar\omega}(E-\hbar\omega)} \tag{9}$$

Given an effective IMFP, we can then infer a lifetime τ for the excitation by dividing the IMFP by the group velocity $(\mathrm{d}\omega_q/\mathrm{d}q)$. This derivative is evaluated based on the dispersion relation predicted by the Mermin formalism at the relevant point of energy and momentum. The lifetime τ is then inversely proportional to the broadening parameter $\gamma(\omega,q) = \hbar/\tau$, which we therefore define at any given combination of energy and momentum

$$\gamma(\omega, q) = \frac{\hbar^2}{a_o\pi E}\frac{\mathrm{d}\omega_q}{\mathrm{d}q}\bigg|_{\omega,q}\int_0^{\omega-\omega_F}\int_{q_-^*}^{q_+^*}\frac{1}{q}\,\mathrm{Im}\left[\frac{-1}{\varepsilon(q,\omega')}\right]\mathrm{d}q\,\mathrm{d}\omega' \tag{10}$$

The width $\gamma_i(q)$ for a particular oscillator i is then related to this generalized broadening function following

$$\gamma_i(q) = \gamma(\omega_q, q) \tag{11}$$

with the special case at the optical limit of $\gamma_i(0) = \gamma(\omega_i,0)$.

In the first instance, calculations are performed using a combination of eqs 1, 5, and 9, building an electron ELF using Lindhard-type FEG functions to approximate the behavior of the solid. This computation is equivalent to the longstanding full Penn algorithm (FPA),[11] which forms the basis of several tabulations currently in the literature.[13] Values for $\gamma_i(q)$ are then obtained used eq 10 to define broadening widths for Mermin functions at all energies and momenta, and a new ELF is built using these functions. The process is then repeated until the electron ELF is converged and therefore self-consistent. Mathematically, we may define this iterative formalism by representing the inverse IMFP as a sum of broadened oscillators with relative strengths A_i

$$\lambda(E)_N^{-1} = \frac{\hbar}{a_o\pi E}\int_0^{(E-E_F)/\hbar}\int_{q_-}^{q_+}\sum_i\frac{A_i}{q} \times \mathrm{Im}\left[\frac{-1}{\varepsilon_M(q,\omega,\gamma_i(q)_{N-1};\,\omega_p=\omega_i)}\right]\mathrm{d}q\,\mathrm{d}\omega \tag{12}$$

This equation can then be generalized by substituting an integral form of eq 4 to obtain

$$\lambda(E)_N^{-1} = \frac{\hbar}{a_o\pi E}\int_0^{(E-E_F)/\hbar}\int_{q_-}^{q_+}\int_0^\infty\frac{2}{\pi}\frac{\omega'}{q} \times \mathrm{Im}\left[\frac{-1}{\varepsilon_{data}(0,\omega')}\right] \times \mathrm{Im}\left[\frac{-1}{\varepsilon_M(q,\omega,\gamma_i(q)_{N-1};\,\omega_p=\omega_i)}\right]\mathrm{d}\omega'\,\mathrm{d}q\,\mathrm{d}\omega \tag{13a}$$

$$\gamma_i(q)_N = \hbar\frac{\mathrm{d}\omega_q}{\mathrm{d}q}\bigg|_{\omega_q,q}\lambda(E)_N^{-1}\Theta(N-\delta) \tag{13b}$$

where the broadening values $\gamma_i(q)_N$ are given in terms of the IMFP $\lambda(E)_N$ by comparison with eq 10. Θ is the Heaviside step function, and δ is a positive infinitesimal. Successive iterations

DOI: 10.1021/jz5023812
J. Phys. Chem. Lett. 2015, 6, 314–319

of eq 13 generate a coupled-plasmon model of increasing order, with convergence to a self-consistent result typically achieved by $N > 4$.

We have applied this approach to calculating the electron ELFs and free-electron IMFPs in elemental molybdenum and aluminum. Molybdenum is an ideal test case due to the recent experimental interest in the material and its characteristic strongly defined optical resonance peaks.[24] Aluminum, by contrast, is often considered a free-electron-like material, exhibiting a single dominant optical resonance at around 14.5 eV. Figure 1 shows the generalized broadening function $\gamma(\omega,q)$

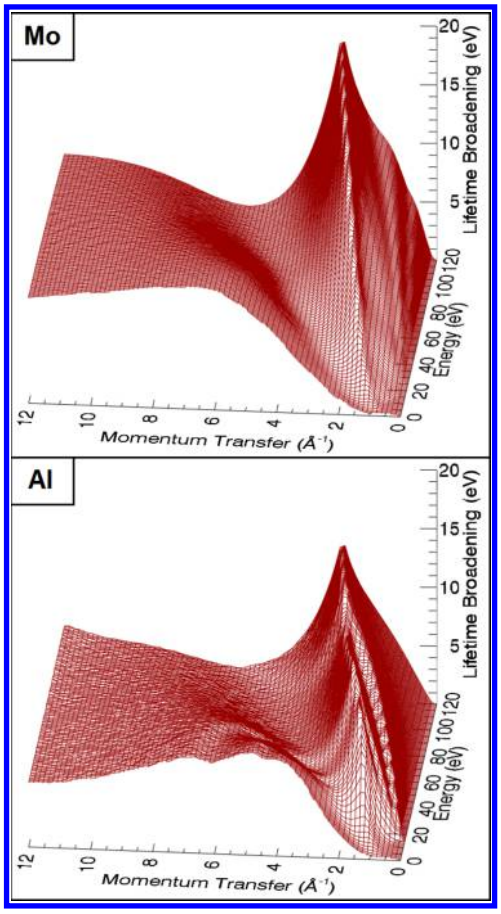

Figure 1. Plasmon and single-electron excitation broadening spectrum for elemental molybdenum and aluminum. Values from this surface are used to determine the lifetime broadening to be applied to the electron ELF, ensuring a physical and self-consistent representation of plasmon coupling in the material.

for all combinations of energy and momentum for both molybdenum (upper pane) and aluminum (lower pane), up to $\hbar\omega = 120$ eV and $\hbar q = 12$ Å^{-1}.

This figure represents the lifetime broadening associated with both free- and bound-state electrons in the solid and has a number of striking physical characteristics. First, in the optical limit, the function always reduces to zero. This is partly due to the vanishing integration range of the ELF given by eq 9 and partly because the group velocity approaches zero for momentum-free excitations (i.e., standing waves). Therefore, the model predicts that a Lindhard-type formalism (i.e., a lossless formalism) is both valid and *required* when $\hbar q = 0$ and that this would be so regardless of how the optical broadening widths were initially defined.

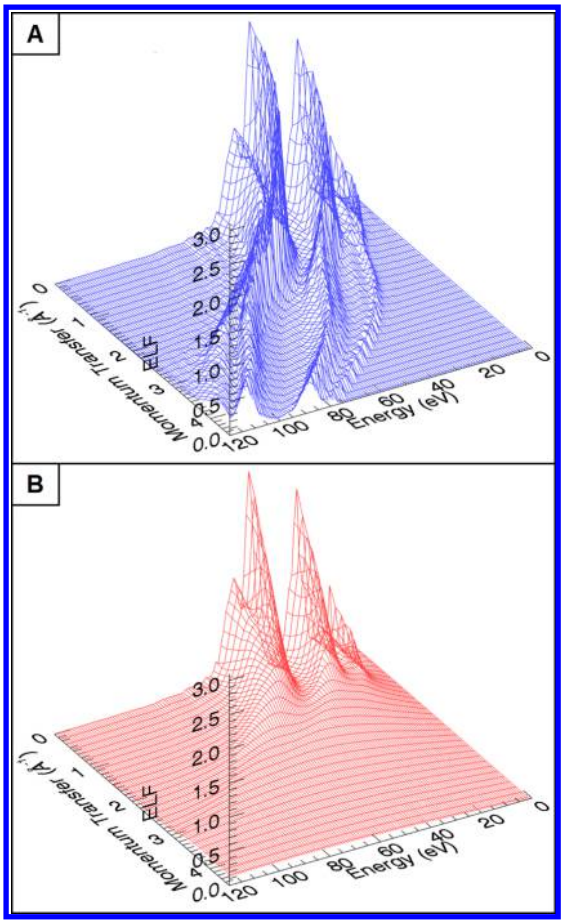

Figure 2. Electron ELF of elemental molybdenum. (A) is calculated using a lossless Lindhard-type model, while (B) utilizes a self-consistent coupled-plasmon model (eq 13) to incorporate excitation broadening following values from Figure 1. In a qualitatively similar fashion to previous Mermin-type modeling,[24] the broadened ELF has much less structure at high momenta but predicts far greater scattering losses at low energies, leading to a lower electron IMFP.

The second striking feature is that a clear trench is formed along a particular path with increasing energy and momentum and that this closely follows the dispersion relation of a free particle. Despite differences in the magnitudes of the broadening for Mo and Al, the trench appears for both materials along the same characteristic path. It makes intuitive sense that an energetic bound particle will have a shorter lifetime due to its strong interaction with the potential of the solid, but it is a compelling property of this model that such a physical insight is directly manifested and material-independent. This feature may be considered a direct analogue of the well-known Bethe ridge, which corresponds to a peak in the electron ELF following the dispersion relation of a free particle at high energies. Unlike the Bethe ridge, however, this feature is well-defined across all energies and therefore may more readily be used as a test of the physicality of the model ELF. The current model appears to be the first to robustly predict such a feature for the general behavior of the scattering material, in particular contrast to recent density functional investigations where radically differing dispersion behavior was predicted for individual excitations.[30]

The particularly high level of broadening observed for excitations with high energy but low momentum is also important as these are excitations that typically exist beyond the

DOI: 10.1021/jz5023812
J. Phys. Chem. Lett. 2015, 6, 314−319

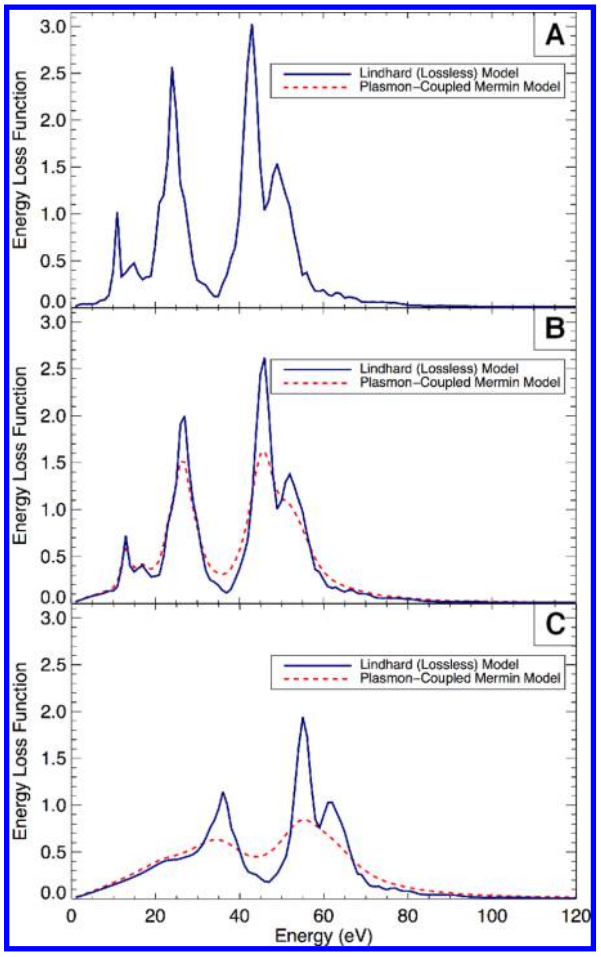

Figure 3. ELF of molybdenum at momentum transfer $\hbar q$ equal to (A) 0, (B) 0.75, and (C) 1.5 Å^{-1}. In the optical limit, both Lindhard and coupled-plasmon models coincide with externally determined optical loss data. At higher momenta, the coupled-plasmon model leads to increased broadening as higher-energy excitations couple into lower-energy excitations.

range of integration used when determining the IMFP of a free particle. This means that although in a lossless Lindhard formalism such excitations would play no part, in the current model, they are valid excitation channels into which the free electron may deposit energy and thus reduce the calculated IMFP.

The detailed behavior of individual resonances is best illustrated by the full energy- and momentum-dependent ELF for molybdenum, which we present in Figure 2. The blue surface is determined using a lossless Lindhard model, while the red mesh uses the current self-consistent model with momentum-dependent broadening as described. In both cases plotted and in our analysis of aluminum, the optical limit of the spectrum is determined externally by DFT calculations.[24,31]

The Lindhard model clearly retains the optical loss structure at higher momentum values, while the self-consistent Mermin spectrum quickly establishes a broad range of potential excitations that persist at very low energies. This leads to a significant increase in the scattering and thus a decrease in the IMFP of low-energy electrons without a significant impact on high-energy electrons. In Figure 3, we show cross sections of the electron ELF for molybdenum at three different values of the momentum transfer $\hbar q$.

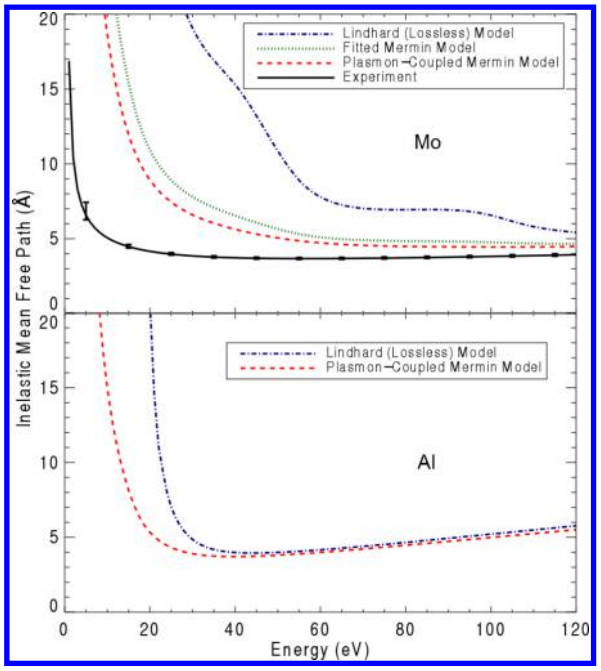

Figure 4. Theoretical and experimental determinations of the electron IMFP for molybdenum and aluminum. The solid black curve with uncertainties shows a recent high-precision Mo measurement from XAFS,[6] while the green dotted curve uses a more traditional fit-based Mermin modeling. The blue dotted–dashed curves show results from a lossless Lindhard-type representation of the electron ELF, while the red dashed curves use the current coupled-plasmon model defined by eq 13. The implementation of self-consistent excitation broadening has a dramatic effect on the IMFP for molybdenum due to its broad loss spectrum and many excitation channels, while the reduction for aluminum is far more modest due to its singly resonant loss structure.

This figure shows one of the most important physical properties of the model, that excitations at higher energies have a greater level of broadening as the energy from these resonances may be coupled into lower-energy excitations. We therefore call this a coupled-plasmon model as it intrinsically accounts for the interaction between different plasmon excitations in the medium and relaxes the longstanding approximation that a solid is a collection of noninteracting nearly FEGs. Our implementation of excitation broadening, which is energy- and momentum-dependent, self-consistent, uniquely constrained, and sensitive to the band structure of the absorbing material, subsequently has a dramatic effect on the electron IMFP. This is plotted for both molybdenum and aluminum in Figure 4. In the case of molybdenum, we compare the new coupled-plasmon model with a lossless Lindhard model, our previous fit-based Mermin model,[24] and the recent high-precision measurement from X-ray absorption spectroscopy.[6] For aluminum, we demonstrate the relative significance of including plasmon-coupled broadening for a free-electron-like material with a single dominant resonance peak.

The improved theoretical modeling leads to a dramatic reduction in the IMFP for molybdenum and a substantial improvement in the agreement with the experimental result. Although prior improvements have been shown using Mermin functions,[9] including our recent fit-based Mermin model (dotted green curve in Figure 4),[24] this is the first time that such an outcome has been achieved with a constrained, comprehensively physical model. This result demonstrates the validity of the coupled-plasmon approach and the value of

DOI: 10.1021/jz5023812
J. Phys. Chem. Lett. 2015, 6, 314–319

implementation of a properly physical understanding of interaction between different excitation channels within a well-defined condensed matter system.

The reduction for aluminum is also significant at very low energies, but the result converges far more rapidly to the lossless modeling, which has well-established accuracy at higher energies. This is due to the optical loss spectrum of aluminum consisting of only a single peak at 14.5 eV, meaning that this resonance may only couple into itself at lower-energy states, and there are no significant peaks to broaden at higher energies. Consequently, we demonstrate that a lossless modeling is largely sufficient for aluminum for energies above around 40 eV.

This work aids strongly in the development of IMFP theory in terms of evaluating the relative importance of physical deficiencies in previous modeling. We have been able to confirm for molybdenum that further effects of exchange and correlation are relatively minor above around 50 eV, but of course, they may be dominant for low electron energies. We have shown further that the solid-state band structure of the material is a critical determinant of the significance of excitation broadening in the low-energy regime. The work enables for the first time an approach that includes excitation lifetimes without the need for arbitrary fitting algorithms, meaning that the inclusion of broadening parameters can become standard practice for IMFP determinations. This represents a significant step forward in the understanding of electron transport in general condensed matter systems and is directly and immediately applicable to all current low-energy electron spectroscopies and microscopies.

AUTHOR INFORMATION

Corresponding Author

*E-mail: chantler@unimelb.edu.au.

Notes

The authors declare no competing financial interest.

ACKNOWLEDGMENTS

The authors acknowledge the work of Z. Barnea, M. D. de Jonge, N. A. Rae, and J. L. Glover and their helpful contribution to the development of ideas important to this research.

REFERENCES

(1) Egerton, R. F. Electron energy-loss spectroscopy in the TEM. *Rep. Prog. Phys.* **2009**, *72*, 016502.
(2) Barrett, N.; Krasovskii, E. E.; Themlin, J.-M.; Strocov, V. N. Elastic scattering effects in the electron mean free path in a graphite overlayer studied by photoelectron spectroscopy and LEED. *Phys. Rev. B* **2005**, *71*, 035427−035436.
(3) Bourke, J. D.; Chantler, C. T.; Witte, C. Finite difference method calculations of X-ray absorption fine structure for copper. *Phys. Lett. A* **2007**, *360*, 702−706.
(4) Zhu, Y.; Inada, H.; Nakamura, K.; Wall, J. Imaging single atoms using secondary electrons with an aberration-corrected electron microscope. *Nat. Mater.* **2009**, *8*, 808.
(5) Bourke, J. D.; Chantler, C. T. Measurements of electron inelastic mean free paths in materials. *Phys. Rev. Lett.* **2010**, *104*, 206601−206604.
(6) Chantler, C. T.; Bourke, J. D. X-ray spectroscopic measurement of photoelectron inelastic mean free paths in molybdenum. *J. Phys. Chem. Lett.* **2010**, *1*, 2422.
(7) Chantler, C. T.; Bourke, J. D. Electron inelastic mean free path theory and density functional theory resolving discrepancies for low-energy electrons in copper. *J. Phys. Chem. A* **2014**, *118*, 909.
(8) Nagy, I.; Echenique, P. M. Mean free path of a suddenly created fast electron moving in a degenerate electron gas. *Phys. Rev. B* **2012**, *85*, 115131.
(9) Da, B.; Shinotsuka, H.; Yoshikawa, H.; Ding, Z. J.; Tanuma, S. Extended Mermin method for calculating the electron inelastic mean free path. *Phys. Rev. Lett.* **2014**, *113*, 063201.
(10) Chantler, C. T.; Bourke, J. D. Momentum-dependent lifetime broadening of electron energy loss spectra: Sum rule constraints and an asymmetric rectangle toy model. *Phys. Rev. B* **2014**, *90*, 174306.
(11) Penn, D. R. Electron mean-free-path calculations using a model dielectric function. *Phys. Rev. B* **1987**, *35*, 482−486.
(12) Tung, C. J.; Ashley, J. C.; Ritchie, R. H. Electron inelastic mean free paths and energy losses in solids II. *Surf. Sci.* **1979**, *81*, 427−439.
(13) Tanuma, S.; Powell, C. J.; Penn, D. R. Calculations of electron inelastic mean free paths. IX. Data for 41 elemental solids over the 50 eV to 30 keV range. *Surf. Interface Anal.* **2011**, *43*, 689.
(14) Nikjoo, H.; Uehara, S.; Emfietzoglou, D. Interaction of radiation with matter. *Interaction of Radiation with Matter*; CRC Press: Boca Raton, FL, 2012.
(15) Lindhard, J. On the properties of a gas of charged particles. *Mat.-Fys. Medd. - K. Dan. Vidensk. Selsk.* **1954**, *28*, 1−57.
(16) Mermin, N. D. Lindhard dielectric function in the relaxation-time approximation. *Phys. Rev. B* **1970**, *1*, 2362.
(17) Werner, W. S. M.; Glantschnig, K.; Ambrosch-Draxl, C. Optical constants and inelastic electron-scattering data for 17 elemental metals. *J. Phys. Chem. Ref. Data* **2009**, *38*, 1013.
(18) Hagemann, H.-J.; Gudat, W.; Kunz, C. *Deutsches Elektronen-synchrontron Report SR-74/7*; 1974; pp 1−96.
(19) Palik, E. D. Handbook of Optical Constants of Solids III. Chapter 7 *Handbook of Optical Constants of Solids III*; Academic Press: New York, 1998; pp 187−227.
(20) Vos, M. Extracting detailed information from reflection electron energy loss spectra. *J. Electron Spectrosc. Relat. Phenom.* **2013**, *191*, 65.
(21) Smith, D. Y.; Shiles, E. Finite-energy f-sum rules for valence electrons. *Phys. Rev. B* **1978**, *17*, 4689.
(22) Bourke, J. D.; Chantler, C. T. Electron energy loss spectra and overestimation of inelastic mean free paths in many-pole models. *J. Phys. Chem. A* **2012**, *116*, 3202.
(23) Denton, C. D.; Abril, I.; Garcia-Molina, R.; Moreno-Marin, J. C.; Heredia-Avalos, S. Influence of the description of the target energy-loss function on the energy loss of swift projectiles. *Surf. Inter. Anal.* **2008**, *40*, 1481−1487.
(24) Chantler, C. T.; Bourke, J. D. Full-potential theoretical investigations of electron inelastic mean free paths and extended X-ray absorption fine structure in molybdenum. *J. Phys.: Condens. Matter* **2014**, *26*, 145401.
(25) Ninham, B. W. Plasmon damping in metals. *Phys. Rev.* **1966**, *145*, 209.
(26) Ashley, J. C.; Ritchie, R. H. The influence of damping on the mean free path of low energy electrons in an electron gas. *Phys. Status Solidi* **1977**, *83*, K159.
(27) Nguyen-Truong, H. T. Energy-loss function including damping and prediction of plasmon lifetime. *J. Electron Spectrosc. Relat. Phenom.* **2014**, *193*, 79.
(28) Emfietzoglou, D.; Cucinotta, F. A.; Nikjoo, H. A complete dielectric response model for liquid water: A solution of the Bethe ridge problem. *Radiat. Res.* **2005**, *164*, 202.
(29) Silkin, V. M.; Chulkov, E. V.; Echenique, P. M. First-principles calculation of the electron inelastic mean free path in Be metal. *Phys. Rev. B* **2003**, *68*, 205106.
(30) Alkauskas, A.; Schneider, S. D.; Hebert, C.; Sagmeister, S. Dynamic structure factors of Cu, Ag, and Au: Comparative study from first principles. *Phys. Rev. B* **2013**, *88*, 195124.
(31) Blaha, P.; Schwarz, K.; Madsen, G. K. H.; Kvasnicka, D.; Luitz, J. *WIEN2k - An augmented plane wave plus local orbitals program for calculating crystal properties*; Vienna University of Technology: Vienna, Austria, 2001.

DOI: 10.1021/jz5023812
J. Phys. Chem. Lett. 2015, 6, 314−319